Global NEST Journal, Vol 25, No 1, pp 6-16

Batch and column studies on removal of eriochrome black T dye by microalgae biochar

Thillainayagam B.P.[1,2], and Nagalingam R.[1,2]*

[1]Department of Civil Engineering, Anna University, University College of Engineering, Ramanathapuram 623 513, Tamil Nadu, India
[2]Department of Civil Engineering, Mount Zion College of Engineering and Technology, Pudukkottai, 622 507, Tamil Nadu, India
Received: 30/08/2022, Accepted: 03/10/2022, Available online: 31/10/2022
*to whom all correspondence should be addressed: e-mail: vng.radha@gmail.com, radha.n@mountzion.ac.in
https://doi.org/10.30955/gnj.004444

Graphical abstract

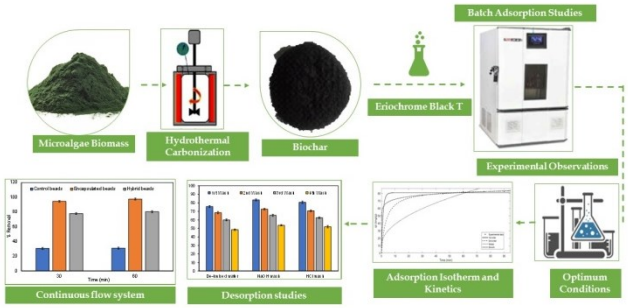

Abstract

In this study, *Chlorella vulgaris* microalgae was cultivated from wastewater and converted into biochar through hydrothermal carbonization process. Acclimatization of microalgae resulted in a greater biomass yield of 4.1 g/L in 15 days in a Fog's medium to wastewater ratio of 20:80. Microalgae biomass was converted into biochar through hydrothermal carbonization process at temperature of 350 °C. The batch adsorption studies for the removal of Eriochrome Black T dye (EBT) from aqueous solution was performed by modifying various parameters. At an initial dye concentration of 100 ppm, a contact time of 60 min, a temperature of 30 °C, a biochar dosage of 0.3 g, and a pH of 7, the best dye removal efficiency was 82.31%. The investigation of the adsorption isotherm and kinetics revealed that the adsorption process followed pseudo-second order kinetics with the Langmuir isotherm model. In addition, the column adsorption investigations were carried out by varying the beads and bed height. Encapsulated beads outperformed control and hybrid beads in terms of removal efficiency. Column parameters such as initial metal ion concentration, bed height, and flow rate were optimised using the BDST model.

Keywords: Adsorption, biochar, microalgae, eriochrome black T dye, desorption

1. Introduction

Water pollution is a big issue that requires attention. It occurs when freshwater comes into contact with one or more hazardous substances, such as chemicals and microorganisms. The capacity of water to move quickly from one area to another, such as from drainage systems to a stream, river, or ocean, is the cause for its prevention of contamination. Water pollution endangers human health, and data show that more people are being killed each year because of contaminated water. Experts anticipate that by the year 2050, difficulties requiring freshwater will have multiplied enormously because people only have access to less than 1% of the world's freshwater. Since water is considered a universal solvent, it is vulnerable to getting polluted more easily. Water pollution is caused by chemicals dumped into water bodies by industry, laboratories, farms, and other sources. Cholera, typhoid, and giardia are among the diseases that have been linked to contaminated water in both humans and animals. It can also cause significant environmental damage, resulting in the deterioration of marine life. Pigments and dyes that are discharged into water bodies are important to include among the numerous contaminants. They are frequently organic in origin and have been used in a variety of sectors. More than 100,000 different varieties of dyes are created and used in industries worldwide (Liu *et al.*, 2015).

Particularly, over 7 × 10^5 tonnes of artificial dyes are produced each year (Gürses *et al.*, 2016). With that being said, the volume of effluent produced in these industries are exorbitant and the lack of suitable treatment procedure to thoroughly detoxify the released contaminated water leads to water pollution. These synthetic dyes can infect the eye, trigger allergic reactions. In countries like the US, the utilization of azo dyes that are derived from harmful amines has been prohibited. Azo dyes are most commonly manufactured in the food, textile, paint and leather industries (Ahmad *et al.*, 2020, Peng *et al.*, 2015; Karnjkar *et al.*, 2015; Tripathi and Ranjan,2015). Owing to the complex aromatic nature of these dyes poses a huge menace to the environment and these dyes are also available commercially (Ahuja, 2018). Natural degradation of azo dyes is possible, however, because they are predominately present in water bodies where sunlight penetration is hindered by the dyes, the rate of

degradation is decreased. The presence of dyes in water also reduces the amount of dissolved oxygen. Furthermore, because of low photosynthetic activity and bacterial development, biodegradation of azo dyes is difficult. Dyes are often mutagenic, teratogenic, and carcinogenic, posing significant risks to aquatic life and human health (Sharifpour *et al.*, 2018).

To address this issue, numerous treatment methods for removing dye from bodies of water were developed. They are generally categorized as advanced oxidation (Lebron *et al.*, 2021), biological (Haddad *et al.*, 2018; Yang *et al.*, 2018), and membrane separation processes (Thamaraiselvan *et al.*, 2018; Campo *et al.*, 2018). Other methods used in industry include flocculation (Ahmad *et al.*, 2020), chemical precipitation (Salama *et al.*, 2019), biological oxidation (Sangave and Pandit, 2006), and activated carbon adsorption (Cui *et al.*, 2019). Because of the recalcitrant nature of dyes, these techniques may be less effective and more expensive. Adsorption, on the other hand, has proven to be one of the most often employed methodologies. They are versatile in nature as they can be designed to remove both organic and inorganic pollutants contained in water. Adsorption is a physical separation method in which a solid, commonly referred to as an adsorbent, attracts the components that are present in the fluid phase. The primary downside of this approach is the high cost of adsorbents. Activated carbon has been shown to perform better in terms of high efficiency in many studies (Mo *et al.*, 2018; Rivera-Utrilla *et al.*, 2011). However, because of its high price, various low-cost replacements are being investigated. Most of the time, those adsorbents that are a waste product of a process are examined to eliminate cost concerns and increase waste management. Palm ash (Sharma *et al.*, 2013), sawdust (Ngah and Hanafiah, 2008), rice husk (O'Connor *et al.*, 2018), wasted tea waste (Kumar *et al.*, 2013), and wheat straw (Ali *et al.*, 2012) are some of the adsorbents used.

However, these adsorbents have issues with the efficiency and cost of regeneration. In recent years several low-cost adsorbents are explored and being improvised to make it to commercialization. Various lignocellulose materials have also been investigated for the treatment of several other contaminants (Mo *et al.*, 2018). Due to their low economic value, these are frequently preferred in industries. Similarly, in recent years, algae have demonstrated enormous potential as a raw material for adsorbents. Algae used as adsorbents are sometimes referred to as bio-adsorbents because they are biological materials. In terms of removal capacity and availability, they have a significant advantage over the others. Whether it is micro or macroalgae, they are capable to adapt to various conditions which promise non-depletion. Algae are capable of growing under erratic climatic and water conditions. The mechanism by which they remove the pollutants can be both by metabolic activity exhibited by living organisms and by passive intake. These bio-adsorbents are environmental-friendly, financially effective and have a high potential to serve as a good medium to remove hard chemicals present in the water. Indifferent to the nature of chemicals present in water, the biomass of algae obtained after drying can be stored with ease and perform significantly better than that of living algae (Kim, 2015). owing to these reasons, algae are researched intensively for the function of dye removal and their efficacy to treat various contaminants.

In this study, we are cultivating *Chlorella vulgaris* microalgae in municipal wastewater and employing it under hydrothermal carbonization process to produce biochar which is further then utilized for the adsorptive elimination of Eriochrome black T dye from an aqueous medium. The batch and column adsorption studies are conducted by varying dosages of biochar (0.1–1 g), temperature (30–50 °C), contact time (30–120 min), concentration of dye (10–200 mg/L), pH (3–10), three different beads and varying height (10, 15, 20, and 25 cm) of the column along with isotherm and kinetics study. Furthermore, desorption studies of the spent biochar are performed to analyse the reusability of the biochar.

2. Material and methods

2.1. Wastewater preparation

In this study, municipal wastewater collected from a nearby wastewater treatment facility located in Chennai, Tamil Nadu, India is utilized for the culture of *Chlorella vulgaris* microalgae. The collected municipal wastewater is subjected to separation techniques such as centrifugation and filtration using the filter paper called Whatman No. 40 with 8 mm pore size, to remove unwanted contaminants and solid impurities present in it. The obtained municipal wastewater is then subjected to various biological methods to determine its Chemical Oxygen Demand (COD) (HACH model DRB200) (Pavithra *et al.*, 2020), ammoniacal nitrogen (Zhou and Boyd, 2016) and phosphate concentration (Ma *et al.*, 2017) both before and after the cultivation of microalgae.

2.2. Biomass cultivation and bio-char production

The seed culture of *Chlorella vulgaris* was obtained from the National Chemical Laboratory in Pune, India. According to Rai and Gupta (Raveendra *et al.*, 2015), the *Chlorella vulgaris* algae were first cultivated with absolutely no water in Fog's culture medium. The Fog's culture medium was made up of 0.2 g magnesium sulphate, 1 mL micronutrient, 0.1 g calcium chloride monohydrate, 5 mL Fe-EDTA solution and 0.2 g dipotassium phosphate. With 100 mL of water, 0.18 g of manganese (II) chloride, 0.286 g of boric acid, 22 mg of zinc sulphate, 0.039 g of sodium molybdate dihydrate, and 8 mg of copper sulphate pentahydrate were combined to make the micronutrient solution. In 100 mL hot water, 0.55 g of ferrous sulphate and 0.745 g of Disodium ethylene diamine tetraacetate dehydrate were combined to make the Fe-EDTA solution. Further, the seed culture medium was grown with the surrounding environmental conditions of 30 ± 2°C, 0.4 v/vm CO_2, pH 7, and 12 h illumination with 4000 lux light intensity. In a photo bioreactor, the algae were made to acclimatize into the wastewater by increasing the ratio of wastewater to Fog's medium from 0:100 to 100:0 in an orderly manner. The dewatered biomass was utilised as

inoculum in phases to prevent nutrient interchange among the culture medium and the effluent. According to the methodology, (Guo *et al.*, 2015) the unit used to represent algal growth is dried weight of biomass (gL^{-1}). After recovering the cultivated biomass, it was characterised and used for biochar production.

The hydrothermal carbonization (HTC) technique was employed for converting the algal biomass into bio-char. A closed airtight reactor made of stainless-steel with 250 mL capacity was utilized for the HTC. The HTC was performed under a nitrogen atmosphere by adding 20 g of biomass into the reactor. For 60 minutes, the reactor was filled with 200 mL of water. The reactor conditions were temperature of 350 °C and pressure of 5 MPa. After the slurry was combined with dichloromethane, the biochar was extracted using a separating funnel (Arun *et al.*, 2020). Because higher temperatures result in more ash formation, an optimum level of temperature was chosen. An electric furnace produced the thermal energy necessary for the biomass carbonization. Following the experiment, the reactor was rapidly cooled with cold water and the biochar was then cleaned with deionized water before drying. The obtained biochar was stored in an airtight container and utilized for the adsorption studies of Eriochrome black dye.

2.3. Characterization of biomass and biochar

The moisture and ash content of the biomass and biochar was using proximate analysis. The CHNS content of the biomass and biochar was evaluated by employing the Elemental analyser (Vario EL cube Elementar, Germany) and the calorific value of the biomass was calculated using Eq. (1). In addition to this, the biological composition of the biomass was determined in accordance with the biochemical experiments. Thermogravimetric analysis was carried out in order to research and analyse its behaviour of biomass under various temperature settings.

$$\mathrm{HHV(MJ/Kg)} = 0.338 \times C + 1.428 \times (H - \mathrm{O}/8) \quad (1)$$

2.4. Wastewater preparation

Eriochrome Black T (EBT) Dye (≥ 90.0% anhydrous basis, Sigma-Aldrich) was acquired from Merk, India. A 500-ppm concentrated stock solution was prepared by dispersing accurately weighed 0.5 g of the dye in 1000 mL distilled water. To investigate the effect of dye concentration on the adsorption process, the 500-ppm concentrated dye stock solution was then diluted to obtain a range of concentrations of standard dye solutions. To determine the concentration of the dye stock solutions that had been prepared, a UV-vis spectrophotometer was used. This spectrometer was capable of processing a 618 mm maximum wavelength.

2.5. Batch adsorption studies

Batch equilibrium adsorption studies were implemented in a 250 mL Erlenmeyer flask with varying dosages of biochar (0.1–1g), temperature (30–50°C), contact time (30–120 min), concentration of dye (10–200 mg/L) and pH (3–10). To explore the influence of factors on the adsorption process, one parameter was modified while the other parameters were held constant throughout the experiment. All the experiments were performed out in an incubator with a shaker to aid the adsorption process and to attain equilibrium. After that, the concentration of the EBT (λ_{max} = 218 nm) in the dye solution mixture was discovered by utilizing a UV-vis Spectrophotometer (UV-1800 Shimadzu, Japan) analyzing at a maximum wavelength of 618 nm (Raveendra *et al.*, 2015). The following equation (2) was employed to evaluate the removal percentage of EBT dye at equilibrium:

$$Removal(\%) = \frac{C_o - C_e}{C_o} \times 100 \quad (2)$$

Here, initially the liquid phase dye concentration is Co (mg/L), and the equilibrium liquid phase dye concentration is Ce (mg/L).

2.6. Immobilization of adsorbent and packed column studies

2.6.1. Calcium alginate and hybrid immobilization

Immobilized beads were created by dissolving a 3 % sodium alginate solution in a 0.2 M CaCl2 solution. To form cross-linkage, about 1 g of prepared biochar was combined with 50 mL of sodium alginate solution and 20 mL of 4 percent glutaraldehyde solution, and beads were formed. The hybrid beads were made from a combination of silica–calcium alginate, biochar, and glutaraldehyde as a crosslinker. To make a silica slurry, 20 g of silica was stirred in 60 mL of deionized water, and it is heated to 80 °C. In total, a 3 percent sodium alginate solution was made and stirred for 30 minutes with the silica slurry. To this, 1 g of biochar was added, along with 4 % glutaraldehyde, and beads were made. Empty beads with no adsorbent were prepared for control studies.

2.6.2. Column adsorption studies

In an apparatus known as glass column apparatus (Internal Diameter: 3 cm & Height: 30 cm), the continuous flow column adsorption studies were performed. The two different prepared beads were filled separately in the apparatus in accordance with the varying height (10, 15, 20, and 25 cm) of the column. The wastewater containing EBT dye of known concentration is pumped upward in the column using peristaltic pump which has the ability to pump at a constant flow rate. Here the flow rate is set to 10 mL/min The effluent flow of the wastewater was continued till the process reached equilibrium. Samples were extracted from the effluent flow at various contact time intervals and the concentration of the EBT (λ_{max} = 218 nm) in the dye solution mixture was deciphered from UV-vis Spectrophotometer (UV-1800 Shimadzu, Japan) analyzing at a maximum wavelength of 618 nm (Raveendra *et al.*, 2015). The removal percentage of EBT dye at equilibrium was calculated using Eq. (2).

2.7. Isotherm study

The Langmuir isotherm were fitted to the adsorption experimental data using the MATLAB R2020a programme. Upon further inspection, the freundlich model was also found fitting reasonably. The best fit for the experimental

data was determined based the error (how much lower it was) and correlation coefficient (R^2) values.

Langmuir model

$$\frac{1}{q_e} = \frac{1}{q_e K_L} \cdot \frac{1}{C_e} + \frac{1}{q_m} \quad (3)$$

Freundlich model

$$\log q_e = \log K_F + \frac{1}{n} \log C_e \quad (4)$$

Where q_e (mg/g) represents the quantity of the EBT dye absorbed when sustaining at equilibrium, the adsorbed quantity of EBT dye after reaching saturation is given by q_m (mg/g), C_e (mg/L) represents the equilibrium concentration of EBT dye and Q_{max} (mg/g) represents the peak adsorption capacity. Further, K_L denotes the Langmuir equilibrium constant and K_F (1/g) and n are the Freundlich equilibrium constant. Further the quantity of EBT dye adsorbed while sustaining in equilibrium (q_e) is calculated using Eq. (7).

$$q_e = \frac{C_e - C_o}{m} \times v \quad (5)$$

Where, m, C_o and v are the mass of bio-char, initial dosage and volume of the dye respectively.

2.8. Kinetics study

For the experimental data, MATLAB R2020a software was used to fit Weber-Morris pseudo-first order, Elovich kinetic models and pseudo-second order. Batch experiments with varying concentrations of biochar (0.1–1 g), at a of temperature (30–50 °C), contact time (30–120 min), concentration of the dye was set between10–200 mg/L, and pH (3–10) were implemented to investigate the kinetics.

Pseudo first order

$$q_t = q_e\left(1 - exp\left(-k_1 t\right)\right) \quad (6)$$

Pseudo second order

$$q_e = \frac{q_e^2 k_2 t}{1 + q_e k_2 t} \quad (7)$$

Webber-Morris model

$$q_e = k_p t^{\frac{1}{2}} + C \quad (8)$$

Elovich model

$$q_e = (1 + \beta_E) \times \ln(1 + \alpha_E \beta_E t) \quad (9)$$

Where, k_1 (1/min), k_2 (g/mg. min) and k_p (mg/g. $min^{1/2}$) are the Pseudo-first order, Pseudo-second order and Webber-Morris constants respectively. Furthermore, C denotes the intercept and q_t (mg/g) denotes the adsorption capacity.

2.9. Desorption study

As the process of removing EBT dye is complete, the spent biochar is studied for its desorption capability using hydrochloric acid (HCl), de-ionized water (H_2O) and sodium hydroxide (NaOH) solutions. About 1 g of the spent adsorbent was dispersed into a 250 mL Erlenmeyer flask which has three different desorption solutions separately adding up to 100 mL. This mixture was stirred for 1 h at normal room temperature. Followed by which the desorbed adsorbent was oven-dried after being separated from the mixture. After that, the concentration of the EBT (λ_{max} = 218 nm) in the mixture was deciphered by using a UV-vis Spectrophotometer (UV-1800 Shimadzu, Japan) analyzing at a maximum wavelength of 618 nm (Raveendra *et al.*, 2015). The desorbed adsorbent after being oven-dried was utilized for the next adsorption study cycle.

3. Results and discussion

3.1. Biomass cultivation

In this study, Chlorella vulgaris microalgae were cultured in a medium comprising varying ratios of fog's medium and wastewater. Initially, the algae were cultured in a medium containing absolutely no wastewater and achieved a peak algal growth of 3.8 g/L in 15 days. As the Fog's medium is rich in nutrients, the algal growth rate was higher. This was not the case when wastewater was added to the medium. Figure 1 shows algae growth at various ratios of Fog's medium to wastewater. The figure illustrates that with a rise in wastewater in the medium, the algal growth decreases. Maximum algal growth of 2.7 g/L and 2.9 g/L was achieved for the Fog's medium to wastewater ratio of 90:10 and 80:20 respectively in 15 days. But after this, the algal growth started to increase with the rise in wastewater ratio. The initial decrease could be because of the sudden addition of wastewater to the medium that might have caused nutrient hindrance. But, with a further increase in the wastewater ratio, the algal growth increased as the algae acclimatized to the wastewater. This caused the algae to efficiently utilize the nutrient levels in wastewater that are organic, for its growth and achieved a maximal algal growth of 4.1 g/L for the Fog's medium to wastewater ratio of 20:80 in 15 days. This is evident by comparing the ammoniacal nitrogen, phosphate and COD levels in the municipal wastewater before and after algae cultivation as organic nutrients such as ammoniacal nitrogen, phosphate, and COD are required for better growth of algae. The levels of ammoniacal nitrogen, phosphate and COD in the municipal wastewater was 72, 93 and 1355 ppm respectively before algae cultivation and was reduced to 19, 37 and 343 ppm respectively after algae cultivation. In other words, the levels of phosphate, ammoniacal nitrogen and COD in the municipal wastewater was reduced by 73.61, 60.22 and 74.69 % respectively after algae cultivation. Similar studies were performed by Chen *et al.* in which they cultured *Chlorella sorokiniana* AK-1 algae in BG-11 used as a medium and swine wastewater in the ratio of 50:50 and achieved 5.45 g/L of maximum algal growth alongside with phosphate, ammoniacal nitrogen and COD reduction of 92.8, 97.0 and 90.1 % respectively (Chen *et al.*, 2020).

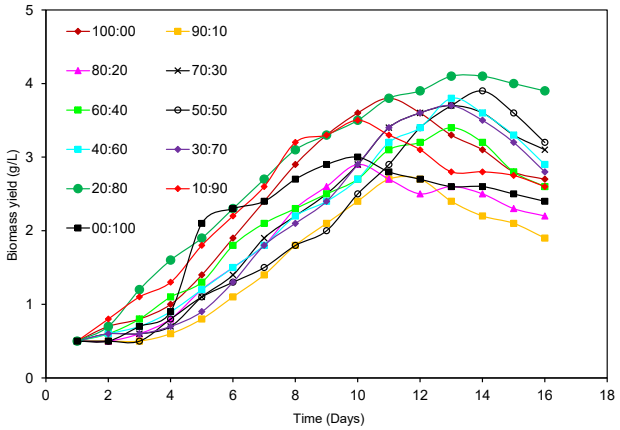

Figure 1. Growth rate of *Chlorella vulgaris* microalgae in a culture medium comprising varying ratios of Fog's medium and municipal wastewater

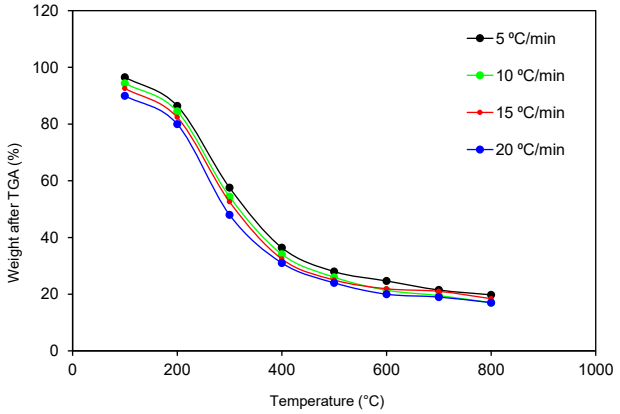

Figure 2. TGA of *Chlorella vulgaris* biomass

3.2. Biomass and biochar characterization

The proximate analysis of the cultivated *Chlorella vulgaris* algae revealed its moisture content to be 10.2 %, volatile content to be 72.6 %, fixed carbon content to be 13.4 % and ash content to be 3.8 %. In the literature, the moisture, volatile compounds, fixed carbon and ash content of the *Chlorella vulgaris* microalgae was found to be 6.78, 82.80, 6.12 and 4.9 % respectively. Furthermore, the carbohydrate, protein and lipid content of the *Chlorella vulgaris* microalgae was found to be 27.46, 34.76 and 21.24% respectively. The biological composition of the algae correlated with its high volatile content. The elemental composition of the *Chlorella vulgaris* microalgae was determined to be Carbon (48.3 %), Hydrogen (5.8 %), Nitrogen (5.4 %), Sulphur (0.8 %) and Oxygen (39.7 %) with a calorific value of 17.52 MJ/kg. In literature, the elemental composition of *Chlorella vulgaris* microalgae was found to be Carbon (47.62 %), Hydrogen (6.99 %), Nitrogen (11.56 %), Sulphur (0.71 %) and Oxygen (24.84 %) with a low calorific value of 21.55 MJ/kg (Chen *et al.*, 2021). The produced algal biomass was converted into biochar through hydrothermal carbonization. Similarly, the elemental composition of the biochar produced through HTC of the cultivated algal biomass was found to be Carbon (85.7 %), Hydrogen (5.4 %), Nitrogen (0.7 %), Sulphur (0.5 %) and Oxygen (7.7 %). The thermal behaviour of the algal biomass for a temperature range of 100–800 °C was analyzed using a thermogravimetric analyser and the results are depicted in Figure 2. The figure illustrates that the heating rate of 20 °C/min showed efficient biomass degradation that that of the other heating rates. The moisture content present in the biomass was removed below 200 °C after which the organic content present in the biomass was degraded at temperature anywhere between 200–500 °C.

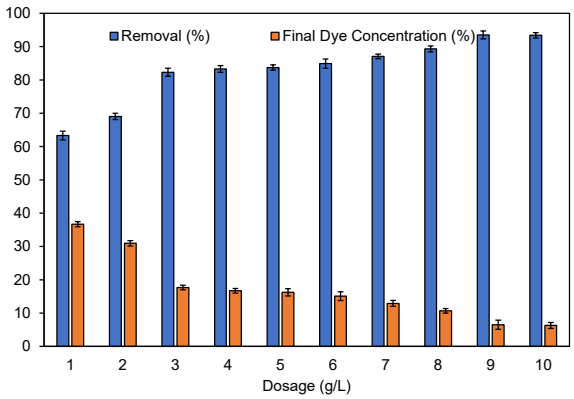

Figure 3. Effect of Biochar dosage on EBT dye removal

3.3. Batch adsorption study

3.3.1. Effect of Biochar dosage on EBT dye removal

By increasing the biochar dosage from 0.1 to 1 g (1–10 g/L), the impact of biochar dosage on the elimination of EBT dye from an aqueous solution was investigated. Other parameters such as pH, initial dye concentration, contact time and temperature were set to of an optimum value of 7, 60 min, 100 ppm and 30 °C respectively. The outcomes of the batch adsorption test on the EBT dye elimination by varying dosage of biochar is depicted in Figure 3. Here, the efficiency of the biochar to adsorb EBT dye rises with an increase in biochar dosage and reaches a maximum of 93.5 % at 9 g/L. The reason is that, with increased biochar dosage, the vacant active sites and surface area available for the adsorbate to attach with the adsorbent increases thereby causing an increase in removal efficiency. But we can see that beyond 9 g/L, the removal efficiency of the biochar decreases by an insignificant amount. In other words, the removal efficiency of the biochar almost becomes constant beyond 9 g/L. Though the maximum removal efficiency is achieved at 9 g/L (93.5 %), we choose 3 g/L (82.31 %) as an efficient one since the removal efficiency that has been increased by a percentage from 3 g/L to 2g/L is tremendous than compared to 9 g/L from 8 g/L. From an industrial point of view, biochar having maximal removal efficiency at lower dosage is preferred to higher dosage as it has the potential to be utilized on large scale. Similarly, Manzar *et al.* reported the effect of adsorbent dosage on the adsorptive removal of congo red and EBT dye from aqueous solution using green coffee residue as adsorbent and achieved maximum removal efficiency at an adsorbent dosage of 40 mg (Chen *et al.*, 2021).

3.3.2. Effect of temperature on ebt dye removal

By adjusting the temperature from 25 to 40 °C, the impact of operation temperature on the elimination of EBT dye from the aqueous solution was investigated. Other parameters such as pH, initial dye concentration, contact time and biochar dosage were set to an optimum value of 7, 60 min, 100 ppm and 0.3 g respectively. The most efficient biochar dosage obtained from the biochar dosage study discussed in the previous section was set as the optimum biochar dosage in this study. Figure 4 gives an overview of batch adsorption tests on the removal of EBT dye at various temperatures. The figure illustrates that the removal efficiency initially increases from 25 °C to 30 °C but plummets beyond 30 °C. The maximum removal efficiency achieved for the adsorption of EBT dye by *Chlorella vulgaris* derived biochar was 82.31 % at 30 °C. As we can see, the maximum removal efficiency is achieved at a lower temperature rather than a higher temperature. This can be attributed to the breaking of electrostatic and intermolecular hydrogen bonding that exist between the adsorbent and adsorbate caused by increased molecular motion at increased temperature. Similarly, Yang *et al.* studied the impact of temperature on the removal efficiency of acid black 172 dye using bamboo-derived biochar and achieved the maximum removal efficiency at 40 °C (Wei, 2014).

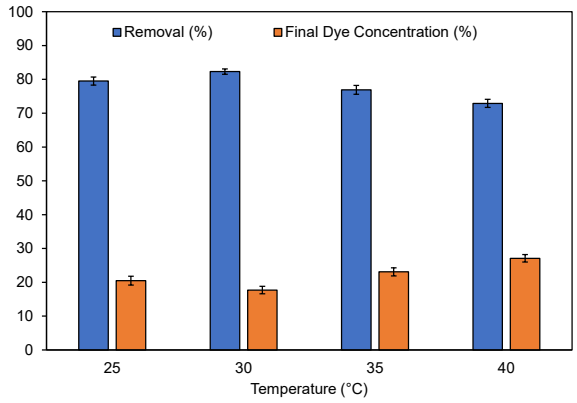

Figure 4. Effect of temperature on EBT dye removal

3.3.3. Effect of contact time on EBT dye removal

By adjusting the contact time from 30 to 90 minutes, the influence of operational contact time on the recovery of EBT dye from the aqueous solution was investigated. pH, temperature, starting dye concentration, and biochar dose were all adjusted to their optimal values of 7, 30 °C, 100 ppm, and 0.3 g, respectively. The most efficient biochar dosage and operating temperature obtained from the effect of biochar dosage and temperature study discussed in the previous sections were set as the optimum condition in this study. The results of the batch adsorption studies on the removal of EBT dye by varying contact time is depicted in Figure 5. The removal efficiency definitely improves with increasing time up to 60 minutes, after which it approaches equilibrium, while there is no further increase in removal efficiency. The maximum removal efficiency achieved for the removal of EBT dye using the *Chlorella vulgaris* derived biochar was 82.31 % at 60 min. This sharp increase could be because of the presence of many active adsorption sites on the adsorbent surface at 30 min that caused the rapid adsorption of EBT dye onto the biochar due to the presence of a large concentration gradient between the solid and liquid interface. With an increase in time, more and more adsorbate gets adsorbed on the adsorbent thereby causing a decrease in the concentration gradient. Beyond a certain point, the number of EBT dye molecules on the solution decreases and reached equilibrium. This is the time at which the removal efficiency gradually decreases and reaches, and stable equilibrium point as seen in the figure after 60 min. Zhang *et al.* studied the influence of contact time on the elimination of methyl orange dye using active biochar derived from pomelo peel waste and obtained similar results with the maximum equilibrium efficiency achieved at 70 min (Zhang *et al.*, 2019).

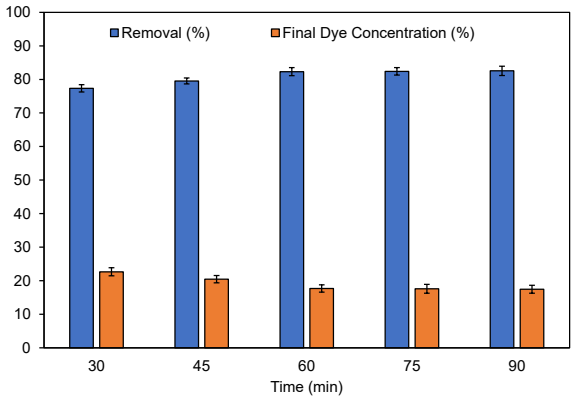

Figure 5. Effect of contact time on EBT dye removal

3.3.4. Effect of initial dye concentration on EBT dye removal

By adjusting the initial dye concentration from 25 to 125 ppm, the effect of initial dye concentration on the removal of EBT dye from the aqueous solution was investigated. pH, temperature, contact time, and biochar dosage were all set to an optimum of 7, 30 °C, 60 min, and 0.3 g, respectively. The most efficient biochar dosage, operating temperature and contact time obtained from the effect of biochar dosage, temperature and contact time study discussed in the previous sections were set as the optimum condition in this study. The outcomes of the batch adsorption studies on the adsorption of EBT dye by varying contact time is depicted in Figure 6. As can be seen from the figure, the removal effectiveness improves as the original dye concentration rises. This could be owing to the high driving force that is imposed by increasing the initial dye concentration. The concentration gradient capable of overcoming the mass transfer barrier between the solid and liquid interface is obtained as the initial dye concentration increases, enhancing the removal efficiency (Ghorbani *et al.*, 2008; Aly-Eldeen *et al.*, 2018). The maximum removal efficiency achieved for the elimination of EBT dye by *Chlorella vulgaris* derived biochar was 82.31 % at 100 ppm. Wen *et al.* observed similar results when investigating the removal efficiency of EBT dye using sludge derived activated carbon (Black, 2019).

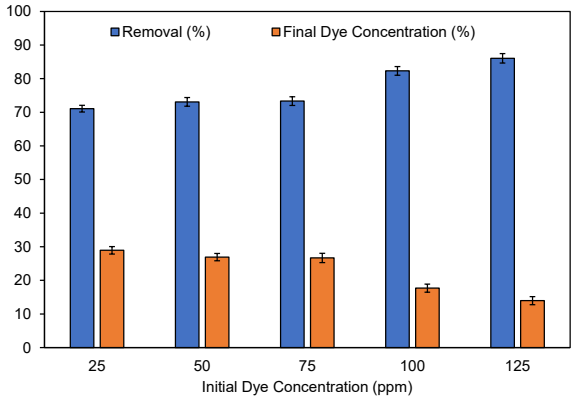

Figure 6. Effect of initial dye concentration on EBT dye removal

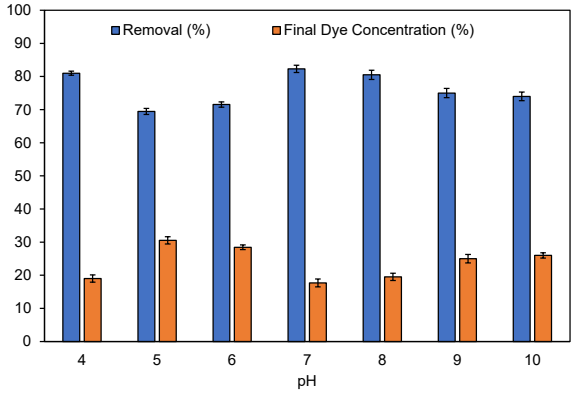

Figure 7. Effect of pH on EBT dye removal

3.3.5. Effect of pH on EBT dye removal

By altering the pH of the solution from 4 to 10, the influence of the pH on the elimination of EBT dye from the aqueous solution was investigated. Initial dye concentration, temperature, contact time, and biochar dosage were all set to their optimal values of 100 ppm, 30°C, 60 min, and 0.3 g, respectively. The most efficient biochar dosage, operating temperature, contact time and initial dye concentration obtained from the effect of biochar dosage, temperature, contact time and initial dye concentration study discussed in the previous sections were set as the optimum condition in this study. The results of the batch adsorption studies are depicted in Figure 7. From the figure, it could be deciphered that the maximum removal efficiency is achieved at pH 4 and 7. The reason for elevated adsorption is that the dissociation of the dye molecules depends on the pH. The surface of the biochar is primarily populated by positively charged ions at acidic pH. As EBT dye is an anionic dye, the surface of the dye is predominantly populated by negatively charged ions. As a result, there is a high electrostatic contact across the adsorbate and the adsorbent at acidic pH, leading in maximum EBT dye removal. With a rise in pH, the quantity of positively charged ions on the surface of the biochar plummets and the quantity of negatively charged ions inclines positively. This negative charge repels the charges present on the dye molecule, thereby causing a decrease in the removal efficiency. At slightly basic pH, the functional group present in the biochar is slightly ionised, which improves dye molecule penetration into the adsorbent. However, further increases in pH create repulsion due to equal electrical charges on the surface of the adsorbent and adsorbate. Thus, optimum adsorption of 82.31 % is observed at pH 7. For all other experiments, pH 7.0 is utilised because it is thought to be closer to the pH of industrial effluents. Similarly, Zubair et revealed the role of pH on the adsorptive removal of anionic dyes Methyl orange and Eriochrome Black T employing biochar generated from the waste Date Palm Fronds and discovered that the biochar's removal efficacy was best at acidic pH (Zubair *et al.*, 2020).

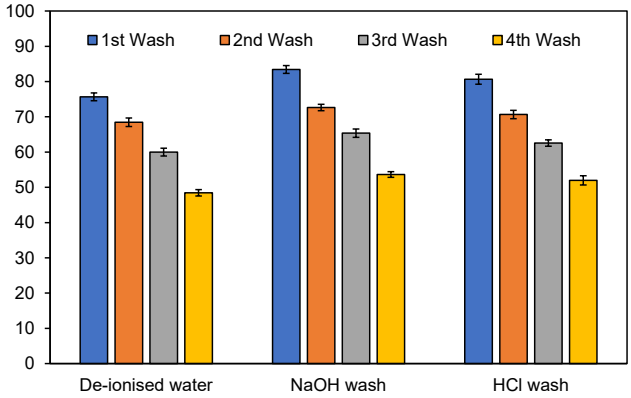

Figure 8. Desorption studies

3.4. Desorption studies

The utility of the adsorbent utilised is governed by various criteria, including the adsorbent's efficiency in removing the required substance, the adsorbent's ability to desorb the most amount of substance that must be adsorbed, but also many other factors. As a result, the biochar must well be able to get recycled as it is a crucial factor to consider for the overall performance of the biochar to eliminate the dye. Several elutants, as shown in Figure 8, could be employed to release the dye from the biochar. Figure 9 depicts the removal of the EBT dye from the biochar using HCl, de-ionized water, and NaOH. Experiments, in which biochar is regenerated four times, were conducted to measure the effectiveness of biochar and the variation of desorption efficacy across all four cycles. The graph clearly shows that as the frequency of washes increases, desorption efficiency declines. When NaOH was utilized as the elutant, 83.43 % of the adsorbed dye was desorbed on the first wash followed by 72.64, 65.36 and 53.65 % on the second, third and fourth wash respectively. Similarly, with HCl as the elutant, a desorption efficiency of 80.64, 70.65, 62.56 and 51.98 % was obtained on the first, second, third and fourth washes respectively. Similarly, with de-ionized water as the elutant, a desorption efficiency of 75.65, 68.46, 60 and 48.45 % was obtained on the first, second, third and fourth washes respectively. Although the desorption efficacy declines with rise in the number of washes with all the elutants, NaOH elutant has the best desorption efficiency even after 4 washes when compared to the HCl elutant and de-ionized water elutant. The reason for increased desorption efficiency with the NaOH elutant is that the biochar is negatively charged due to the adsorption of anionic EBT dye. Hence, when a negatively charged elutant is used for the desorption process, the negative charges on the elutant repels the negative charges

populated on the biochar thereby causing the EBT dye molecules to desorb efficiently. Henceforth, the best elutant apt to desorb EBT dye molecules from the biochar can be NaOH. Islam *et al.* experimented on the desorption studies using EDTA and de-ionized water as elutants on cationic and anionic dyes. They obtained a good desorption efficiency until the third wash with results similar to ours (Islam *et al.*, 2021).

Table 1. Detailed report on adsorption isotherm model for EBT removal

Isotherm Model	SSE	R2	DFE	Adj. R2	RMSE	Coeff.
Freundlich	3.40	0.9728	3	0.96	1.06	2
Langmuir	3.95	0.9683	3	0.96	1.15	2

Table 2. Detailed report on adsorption kinetics model for EBT removal

Kinetic model	SSE	R2	Adj. R2	RMSE
Pseudo first order	21.43	0.9961	0.9951	2.31
Pseudo second order	1.11	0.9998	0.9997	0.53
Elovich	1.89	0.9997	0.9996	0.69
Weber-Morris	711.66	0.8698	0.8373	13.34

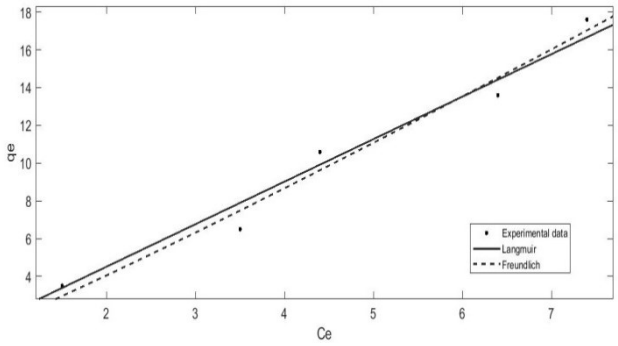

Figure 9. Isotherm Graph for the adsorption of EBT

3.5. Adsorption isotherm

In the present study, two of the most commonly used isotherm models (Langmuir and Freundlich) are employed to study how EBT dye is adsorbed onto the biochar using MATLAB R2020a. These two isotherm models are employed owing to their easy usage, simplicity, and to deduce clear physical meaning while correctly interpreting the obtained data. Of the two employed isotherm models, the perfect fit for the present study is verified with the help of the R^2 value. The parameters like error values (RMSE (root mean square error) and SSE (Sum of squared error)), coefficient values (R^2) calculated for the two isotherm models are depicted in Table 1. The closer the value of the correlation coefficient (R^2) is to unity, the more apt that model is for the study. From data, we can see that the Langmuir isotherm model is suitable for the study with an R^2 value of 0.9728 than the Freundlich isotherm model with an R^2 value of 0.9683. In literature, it has been reported that the Langmuir isotherm model is suitable when the adsorption occurs on the homogeneous surface with an equal adsorption rate (Xie *et al.*, 2019). Henceforth, we can state that the elimination of EBT dye using biochar occurred via monolayer adsorption mechanism with the adsorption energy being uniform throughout the surface of the biochar in which the dye has been adsorbed upon at constant temperature.

3.6. Adsorption kinetics

Kinetic models were exploited to analyse and investigate the mechanism by which EBT dye molecules are adsorbed around on biochar surface. In this study, four kinetics models namely Pseudo-first order, Pseudo-second order, Elovich and Weber-Morris kinetics models were fitted for the experimental data using MATLAB R2020a. The plots obtained for the four-kinetics model are depicted in Figure 10 and the correlation coefficient value (R^2), SSE and RMSE values are illustrated in Figure 2. From the data, it can be seen that the kinetics model fit in the following order: Pseudo-second order > Elovich > Pseudo-first order > Weber-Morris kinetic model with a correlation coefficient (R^2) value of 0.9998, 0.9997, 0.9961 and 0.8373 respectively. As a result, the pseudo-second order model clearly explicates the adsorption mechanism (Table 2). In accordance with the literature (Zubair *et al.*, 2020), the fitting of pseudo-second order model elaborates that the adsorption mechanism of the EBT dye onto the biochar may be due to the chemisorption process involving chemical reaction, electrostatic and π–π interaction between the dye molecule and the biochar's surface.

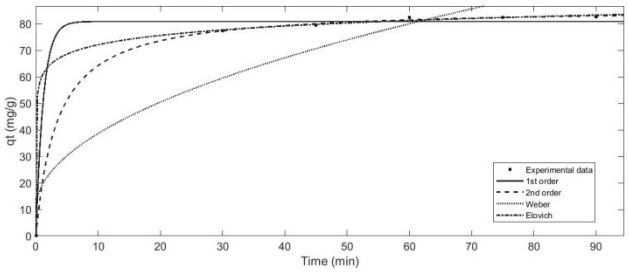

Figure 10. Validation of kinetics model for EBT removal

3.7. Column studies

3.7.1. Effect of bead type

When compared to the immobilised beads, the adsorbent free beads had a negligible degree of dye removal efficiency. This demonstrated that the immobilising substance does not participate in any dye removal mechanism. The batch experimental findings were employed to analyse adsorption efficiency and behaviour of adsorbent material. However, the results from batch

adsorption experiments could not be used to provide scale-up data for commercial treatment systems, whereas continuous flow system (column) studies were typically used for scale-up. The results of the column adsorption studies performed using encapsulated and hybrid beads are illustrated in Figure 11. The figure illustrates that the encapsulated beads have the highest efficiency to remove EBT dye from its solution at both time intervals. The control bead has a removal efficiency of 30.54 and 31.02 % at 30 and 60 min respectively. Similarly, the encapsulated beads have a removal efficiency of 94.5 and 97.6 % at 30 and 60 min respectively. The hybrid beads have a removal efficiency of 77.9 and 80.4 % at 30 and 60 min respectively. When compared to control beads and hybrid beads, the encapsulated beads showed higher removal efficiency and is used in further experiments.

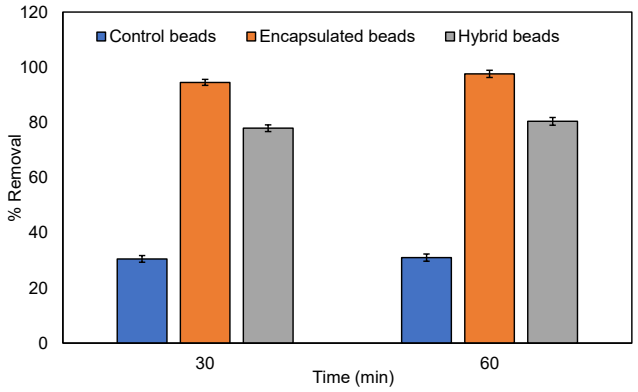

Figure 11. Removal efficiency of various bead type

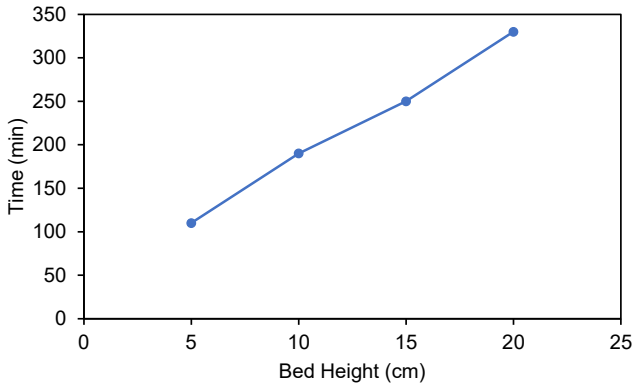

Figure 12. BDST model plot for the removal of EBT dye

3.7.2. Bed-depth service time model

In the present study, the Bed-depth Service Time (BDST) model was employed to study the efficiency of encapsulated beads to remove EBT dye at different time intervals (Figure 12). The dynamic behaviour of a column is explained by the BDST model. The model also illustrates the adsorption process under investigation, with internal and exterior diffusions limited. At a flow rate of 15 mL/min, the graph was generated between Time (min) and bed height (cm). The slope of the BDST graph was used to evaluate the adsorption effectiveness of the bed per unit volume (N_o). The intercept of the plot was used to compute the rate constant, K_a. The rate of solute movement from those in the liquid phase to the solid phase was calculated using the rate constant (Ka). Here, the N_o and K_a for the removal of EBT dye was ____ mg/mL and ___ L/mg h. The BDST model research aids in the flow rate scaling procedure without the need for experimental runs. Because of the greater concentration difference between the metal ions that is contained in the liquid phase and the adsorbent that is present in the solid phase, the adsorption capacity of metal ions was relatively higher in the column study than in the batch study.

4. Conclusion

The Chlorella vulgaris microalgae acclimatized well into the municipal wastewater and achieved a maximal algal growth of 4.1 g/L in 15 days in a culture medium containing Fog's medium to wastewater ratio of 20:80. Biochar was effectively produced from the cultivated microalgae through the hydrothermal carbonization process and the obtained biochar was utilized for batch and column adsorption studies. The batch adsorption studies for the extraction of EBT dye from its aqueous solution was performed by varying several parameters and the best removal efficiency of about 82.31 % was achieved for the operating parameters of 100 ppm initial dye concentration, 60 min contact time, 30 °C temperature, 0.3 g biochar dosage and 7 pH. According to the desorption studies, the NaOH elutant has the highest desorption effectiveness even after 4 washes when compared to the HCl elutant and de-ionized water elutant. The adsorption isotherm and kinetics study revealed that the adsorption process followed pseudo-second order kinetics with the Langmuir isotherm model. Furthermore, the column adsorption studies were performed by modifying the beads and bed height. When compared to control beads and hybrid beads, the encapsulated beads showed higher removal efficiency. The BDST model was used to optimise column parameters such as initial metal ion concentration, bed height, and flow rate.

References

Ahmad T., Belwal T., Li L., Ramola S., Aadil R.M., Xu Y., *et al.* (2020). Utilization of wastewater from edible oil industry, turning waste into valuable products: A review. *Trends in Food Science & Technology,* **99**, 21–33.

Ahuja S. (2018). Advances in Water Purification Techniques: Meeting the Needs of Developed and Developing Countries. Elsevier.

Ali I., Asim M., and Khan T.A. (2012). Low cost adsorbents for the removal of organic pollutants from wastewater. *Journal of Environmental Management,* **113**, 170–183.

Aly-Eldeen M.A., El-Sayed A.A.M., Salem D.M.S.A., and El Zokm G.M. (2018). The uptake of Eriochrome Black T dye from aqueous solutions utilizing waste activated sludge: Adsorption process optimization using factorial design. *Egyptian Journal of Aquatic Research,* **44**, 179–186.

Arun J., Gopinath K.P., SundarRajan P., Malolan R., and AjaySrinivaasan P. (2020). Hydrothermal liquefaction and pyrolysis of Amphiroa fragilissima biomass: comparative study on oxygen content and storage stability parameters of bio-oil. *Bioresource Technology Reports*. **11**, 100465.

Black T. (2019). Preparation of Sludge-Derived Activated Carbon by Fenton Activation and the Adsorption of Eriochrome. https://doi.org/10.3390/ma12060882.

Campo R., Corsino S.F., Torregrossa M., and Di Bella G. (2018). The role of extracellular polymeric substances on aerobic granulation with stepwise increase of salinity. *Separation and Purification Technology*, **195**, 12–20.

Chen C., Qi Q., Zeng T., Fan D., Zhao J., Qiu H., *et al.* (2021). Effect of compound additive on microwave-assisted pyrolysis characteristics and products of Chlorella vulgaris. *Journal of the Energy Institute,* **98**, 188–198.

Chen C-Y., Kuo E-W., Nagarajan D., Ho S-H., Dong C-D., Lee D-J., *et al.* (2020). Cultivating Chlorella sorokiniana AK-1 with swine wastewater for simultaneous wastewater treatment and algal biomass production. *Bioresource Technology,* **302**, 122814.

Cui Y., Masud A., Aich N., and Atkinson J.D. (2019). Phenol and Cr (VI) removal using materials derived from harmful algal bloom biomass: Characterization and performance assessment for a biosorbent, a porous carbon, and Fe/C composites. *Journal of Hazardous Material*s, **368**, 477–486.

Ghorbani F., Younesi H., Ghasempouri S.M., Zinatizadeh A.A., Amini M., and Daneshi A. (2008). Application of response surface methodology for optimization of cadmium biosorption in an aqueous solution by Saccharomyces cerevisiae. *Chemical Engineering Journal,* **145**, 267–275.

Guo Z., Phooi W.B.A., Lim Z.J., and Tong Y.W. (2015). Control of CO2 input conditions during outdoor culture of Chlorella vulgaris in bubble column photobioreactors. *Bioresource Technology*. **186**, 238–245.

Gürses A., Açıkyıldız M., Güneş K., and Gürses M.S. (2016). Dyes and pigments: their structure and properties. Dye. *Pigment., SpringerBriefs,* p. 13–29.

Haddad M., Abid S., Hamdi M., and Bouallagui H. (2018). Reduction of adsorbed dyes content in the discharged sludge coming from an industrial textile wastewater treatment plant using aerobic activated sludge process. *Journal of Environmental Management,* **223**, 936–946.

Islam T., Peng C., Ali I., Li J., Khan Z.M., Sultan M., *et al.* (2021). Synthesis of Rice Husk-Derived Magnetic Biochar Through Liquefaction to Adsorb Anionic and Cationic Dyes from Aqueous Solutions. *Arabian Journal for Science and Engineering,* **46**, 233–246. https://doi.org/10.1007/s13369-020-04537-z.

Karnjkar Y.S., Dinde R.M., Dinde N.M., Bawankar K.N., Hinge S.P., Mohod A.V., *et al.* (2015). Degradation of magenta dye using different approaches based on ultrasonic and ultraviolet ir-radiations: comparison of effectiveness and effect of addi-tives for intensification. *Ultrason Sonochem*, **27**, 117–124.

Kim S-K. (2015). Handbook of marine microalgae: Biotechnology advances. Academic Press.

Kumar R., Singh D., Gupta R., and Tiwari A. (2013). Egg shell and spent tea: An eco-friendly cost effective adsorbent. *International Journal Biological & Pharmaceutical Research,* **4**, 896–901.

Lebron Y.A.R., Moreira V.R., and de Souza Santos L.V. (2021). Biosorption of methylene blue and eriochrome black T onto the brown macroalgae Fucus vesiculosus: equilibrium, kinetics, thermodynamics and optimization. Environmental Technology, **42**, 279–297.

Liu L., Gao Z.Y., Su X.P., Chen X., Jiang L., and Yao J.M. (2015). Adsorption removal of dyes from single and binary solutions using a cellulose-based bioadsorbent. *ACS Sustainable Chemistry & Engineering,* **3**, 432–442.

Ma J., Yuan Y., Zhou T., and Yuan D. (2017). Determination of total phosphorus in natural waters with a simple neutral digestion method using sodium persulfate. Limnol Oceanogr Methods. **15**, 372–380.

Mo J., Yang Q., Zhang N., Zhang W., Zheng Y., and Zhang Z. (2018). A review on agro-industrial waste (AIW) derived adsorbents for water and wastewater treatment. *Journal of Environmental Management*. **227**, 395–405. https://doi.org/10.1016/j.jenvman.2018.08.069.

Ngah W.S.W., and Hanafiah M.A.K.M. (2008). Removal of heavy metal ions from wastewater by chemically modified plant wastes as adsorbents: a review. *Bioresource Technology,* **99**, 3935–3948.

O'Connor D., Peng T., Li G., Wang S., Duan L., Mulder J., *et al.* (2018). Sulfur-modified rice husk biochar: a green method for the remediation of mercury contaminated soil. *Science of the Total Environment*, **621**, 819–826.

Pavithra K.G., Jaikumar V., Kumar P.S., and Sundarrajan P. (2020). Cleaner strategies on the effective elimination of toxic chromium from wastewater using coupled electrochemical/biological systems. *Environmental Progress & Sustainable Energy,* **39**, e13399.

Peng Q., Liu M., Zheng J., and Zhou C. (2015). Adsorption of dyes in aqueous solutions by chitosan–halloysite nanotubes composite hydrogel beads. Microporous Mesoporous Mater, **201**, 190–201.

Raveendra R.S., Prashanth P.A., Malini B.R., and Nagabhushana B.M. (2015). Adsorption of Eriochrome black-T azo Dye from Aqueous solution on Low cost Activated Carbon prepared from Tridax procumbens Adsorption of Eriochrome black-T azo Dye from Aqueous solution on Low cost Activated Carbon prepared from Tridax procumbens.

Rivera-Utrilla J., Sánchez-Polo M., Gómez-Serrano V., Álvarez P.M., Alvim-Ferraz M.C.M., and Dias J.M. (2011). Activated carbon modifications to enhance its water treatment applications. An overview. *Journal of Hazardous Materials*, **187**, 1–23.

Salama E-S., Roh H-S., Dev S., Khan M.A., Abou-Shanab R.A.I., Chang S.W., *et al.* (2019). Algae as a green technology for heavy metals removal from various wastewater. *World Journal of Microbiology and Biotechnology,* **35**, 1–19.

Sangave P.C., and Pandit A.B. (2006). Ultrasound and enzyme assisted biodegradation of distillery wastewater. *Journal of Environmental Management,* **80**, 36–46.

Sharifpour E., Khafri H.Z., Ghaedi M., Asfaram A., and Jannesar R. (2018). Isotherms and kinetic study of ultrasound-assisted adsorption of malachite green and Pb2+ ions from aqueous samples by copper sulfide nanorods loaded on activated carbon: experimental design optimization. *Ultrason Sonochem*, 40, 373–382.

Sharma P.K., Ayub S., Tripathi C.N. Agro and horticultural. (2013). wastes as low cost adsorbents for removal of heavy metals from wastewater: A review. *International Journal of Engineering Science,* **2**, 18–27.

Thamaraiselvan C., Michael N., and Oren Y. (2018). Selective separation of dyes and brine recovery from textile wastewater by nanofiltration membranes. *Chemical Engineering and Technology*, **41**, 185–293.

Tripathi A., and Ranjan M.R. (2015). Heavy metal removal from wastewater using low cost adsorbents. *Journal of Bioremediation & Biodegradation,* **6**, 315.

Wei Y.Y.X.L.B. (2014). Evaluation of adsorption potential of bamboo biochar for metal-complex dye : equilibrium , kinetics and artificial neural network modeling, 1093–10100. https://doi.org/10.1007/s13762-013-0306-0.

Xie Y., Yuan X., Wu Z., Zeng G., Jiang L., Peng X., *et al.* (2019). Adsorption behavior and mechanism of Mg/Fe layered double hydroxide with Fe3O4-carbon spheres on the removal of Pb (II) and Cu (II). *Journal of Colloid and Interface Science,* **536**, 440–455.

Yang B., Xu H., Yang S., Bi S., Li F., Shen C., *et al.* (2018). Treatment of industrial dyeing wastewater with a pilot-scale strengthened circulation anaerobic reactor. *Bioresource Technology,* **264**, 154–162.

Zhang B., Wu Y., and Cha L. (2019). Removal of methyl orange dye using activated biochar derived from pomelo peel wastes : performance , isotherm , and kinetic studies. *Journal of Dispersion Science and Technology,* 1–12. https://doi.org/10.1080/01932691.2018.1561298.

Zhou L., and Boyd C.E. Comparison of Nessler, phenate, salicylate and ion selective. (2016). electrode procedures for determination of total ammonia nitrogen in aquaculture. Aquaculture. **450**, 187–193.

Zubair M., Mu'azu N.D., Jarrah N., Blaisi N.I., Aziz H.A.A. and Al-Harthi M. (2020). Adsorption Behavior and Mechanism of Methylene Blue, Crystal Violet, Eriochrome Black T, and Methyl Orange Dyes onto Biochar-Derived Date Palm Fronds Waste Produced at Different Pyrolysis Conditions. *Water, Air, & Soil Pollution*, **231**. https://doi.org/10.1007/s11270-020-04595-x.